

Parametric mode regression for bounded data

Haiming Zhou^{a*}, Xianzheng Huang^b, and For the Alzheimer's Disease
Neuroimaging Initiative[†]

^aDepartment of Statistics and Actuarial Science, Northern Illinois University

^bDepartment of Statistics, University of South Carolina

June 13, 2022

Abstract

We propose new parametric frameworks of regression analysis with the conditional mode of a bounded response as the focal point of interest. Covariates effects estimation and prediction based on the maximum likelihood method under two new classes of regression models are demonstrated. We also develop graphical and numerical diagnostic tools to detect various sources of model misspecification. Predictions based on different central tendency measures inferred using various regression models are compared using synthetic data in simulations. Finally, we conduct regression analysis for data from the Alzheimer's Disease Neuroimaging Initiative and data from a geological application to demonstrate practical implementation of the proposed methods. Supplementary materials that contain technical details, and additional simulation and data analysis results are available online.

Keywords: Beta distribution; Generalized biparabolic distribution; Linear predictor; Link function; Maximum likelihood.

*Corresponding Author. Email: zhouh@niu.edu

[†]Data used in preparation of this article were obtained from the Alzheimer's Disease Neuroimaging Initiative (ADNI) database (adni.loni.usc.edu). As such, the investigators within the ADNI contributed to the design and implementation of ADNI and/or provided data but did not participate in analysis or writing of this report. A complete listing of ADNI investigators can be found at: http://adni.loni.usc.edu/wp-content/uploads/how_to_apply/ADNI_Acknowledgement_List.pdf

1 Introduction

The statistical models and methodology presented in this article are motivated by the Alzheimer’s Disease Neuroimaging Initiative (ADNI) launched in 2003 and led by Principal Investigator Michael W. Weiner, MD. It is an ongoing study with a public-private partnership in the United States and Canada that gathers and analyzes thousands of subjects’ brain scans, genetic profiles, and biomarkers in blood and cerebrospinal fluid. The main goal of ADNI is to understand relationships among the clinical, cognitive, imaging, genetic and biochemical biomarker characteristics of the entire spectrum of Alzheimer’s diseases (AD). Ultimately, the hope is to achieve early detection of AD in preparation for early intervention of the disease progression, and also to help recruiting appropriate individuals in clinical trials. Clinical outcomes for assessing one’s cognitive function in ADNI are bounded scores from well-established neuropsychological tests, such as the Alzheimer’s disease assessment scale (ADAS, Rosen et al., 1984; Kueper et al., 2018), mini-mental state examination (Tombaugh and McIntyre, 1992), and Rey auditory verbal learning test (Schmidt, 1996). Distributions of these test scores from the ADNI cohort are typically heavy-tailed and skewed. As an example, Figure 1 presents histogram of the ADAS-cognition sub-scale scores, also referred to as ADAS-11, of subjects at month 12 who were diagnosed with late mild cognitive impairment (LMCI) when they entered the ADNI Phase 1 study.

In order to effectively reveal the association between one’s cognitive skill and potential influential biomarkers, we formulate parametric mode regression models tailored for heavy-tailed, skewed, and bounded response data, with efficient prediction as our goal of statistical inference besides identifying influential biomarkers for AD. Under the nonparametric framework, Wang et al. (2017) carried out mode regression analysis of ADNI data to predict cognitive impairment using neuroimaging data. They noted that mean regression analysis for studying the association between the cognitive assessment of an individual and the individual’s neuroimaging features failed to yield scientifically meaningful results due to the heavy-tailed and skewed noise presented in data typically arising in this application. In ad-

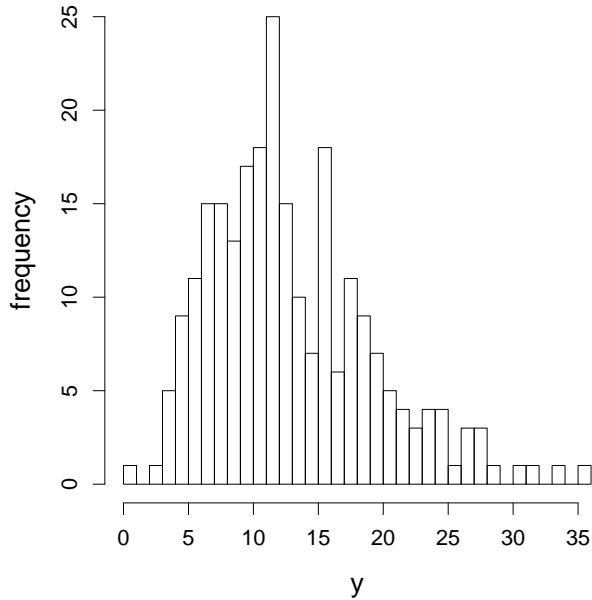


Figure 1: Histogram of ADAS-11 scores at month-12 of subjects in ADNI Phase 1 study.

dition to biomedical applications, mode regression for association study has been routinely used in econometrics (Lee, 1989, 1993; Kemp and Silva, 2012; Damien et al., 2017), astronomy (Bamford et al., 2008), traffic engineering (Einbeck and Tutz, 2006). Kemp and Silva (2012) argued that the mode is the most intuitive measure of central tendency for positively skewed data found in many econometric applications such as wages, prices, and expenditures. More generally, the conditional mode serves as a more informative summary for associations between a response Y and covariates \mathbf{X} than the conditional mean or median when the distribution of Y given \mathbf{X} is heavy-tailed or skewed. When comparing with predictions based on conditional means or medians, predictions based on conditional modes can provide more meaningful estimated outcomes. Yao and Li (2014) showed that, when the interval width is fixed, a mode-based prediction interval tends to have a higher coverage probability than a mean-based prediction interval.

Most existing works on mode regression involve nonparametric components (Yao and Li, 2014; Chen et al., 2016; Zhang et al., 2013; Zhao et al., 2014; Liu et al., 2013; Yang and Yang, 2014). These nonparametric and semiparametric approaches are developed under

the frequentist framework. A few developments under the Bayesian framework include Yu and Aristodemou (2012) and Damien et al. (2017). Even though nonparametric methods and semiparametric methods can protect against misleading inference caused by inadequate parametric assumptions, often at the price of low statistical efficiency, it is not unreasonable to believe that an inference procedure may still provide reliable inference for the mode of a distribution even when certain aspects, such as tails, of the distribution are not well estimated by this procedure (Hall, 1992; Zhou and Huang, 2019). Hence, with the potential gain in efficiency, parametric regression models can be useful in studying the association between a response and covariates via inferring the conditional mode.

Assuming a unimodal conditional distribution for the response, we formulate in Section 2 two new classes of mode regression models for a bounded response. Bounded response data are ubiquitous in practice, with the ADAS-11 score as one example. Other examples include rates or proportions, such as a disease prevalence, the fraction of household income spent on food, and the proportion of food and hygienic waste in residential solid waste. Although, technically, one can often map a bounded response to a new response whose support is the entire real line, say, via a logit transformation for a rate response, and then carry out regression analysis on the new response, it is practically more appealing to directly study the association between the original response and covariates.

Following the model formulation, we outline maximum likelihood estimation of parameters in these models in Section 2. In Section 3 we propose graphical and numerical diagnostics methods for detecting various sources of model misspecification when one draws inference based on an assumed model in the two proposed families. Section 4 presents simulation studies where we carry out mode regression analysis using these assumed models based on data generated from models that may or may not belong to the two families. In these simulation experiments, we report maximum likelihood estimates (MLEs) for covariate effects, operating characteristics of the proposed diagnostics methods, and prediction intervals constructed based on the proposed mode regression models. In Section 5 we carry out mean

and mode regression analysis for a data set from ADNI, and also for another data set from a geological study. Finally, we summarize contributions of this work and discuss follow-up research in Section 6.

2 Two families of regression models and maximum likelihood estimation

2.1 Regression models

Without loss of generality, we assume from now on that the response variable has support on $[0, 1]$, since any other bounded support can be rescaled to the unit interval. For a random variable V that follows a beta distribution, its probability density function (pdf) is given by

$$f_{\text{beta}}(v; \alpha_1, \alpha_2) = \frac{\Gamma(\alpha_1 + \alpha_2)}{\Gamma(\alpha_1)\Gamma(\alpha_2)} v^{\alpha_1-1} (1-v)^{\alpha_2-1}, \quad \text{for } v \in [0, 1], \quad (2.1)$$

where $\Gamma(t)$ is the gamma function, α_1 and α_2 are two positive shape parameters. When $\alpha_1, \alpha_2 > 1$, there is a unique mode for the beta distribution given by $\theta = (\alpha_1 - 1) / (\alpha_1 + \alpha_2 - 2)$. If V follows a generalized bipolar distribution (GBP, García et al., 2009) on the support $[0, 1]$, its pdf is given by

$$f_{\text{GBP}}(v; \theta, m) = \frac{(2m+1)(m+1)}{(3m+1)} d^m (2-d^m), \quad (2.2)$$

where m is a positive shape parameter, and $d = I(0 < v \leq \theta)v/\theta + I(\theta < v \leq 1)(1-v)/(1-\theta)$, in which $\theta \in (0, 1)$ is the mode of the distribution, and $I(\cdot)$ is the indicator function. A larger m leads to a GBP distribution more concentrated around the mode with a smaller variance. Figure 2 depicts three GBP density functions, in comparison with three beta density functions that share the same mode and variance as the corresponding depicted GBP distributions. This figure shows the general pattern that, with the mode and variance

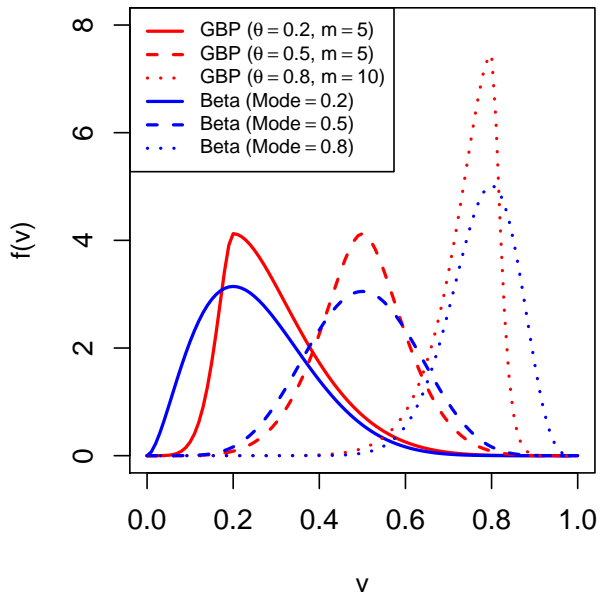


Figure 2: Probability density functions of GBP distributions (red lines) with $(\theta, m) = (0.2, 5)$ (solid line), $(0.5, 5)$ (dashed line), and $(0.8, 10)$ (dotted line), respectively, and beta density curves (blue lines) with the same mode and variance as those of the GBP densities depicted in the same line type.

fixed, a GBP density displays a sharper drop toward zero on both sides of the mode than that for a beta density.

Directly including the mode in the parameterization, as seen in the GBP family, makes it more convenient to draw inference for the mode. For this reason, we reparameterize the two shape parameters in the beta density function in (2.1) by setting $\alpha_1 = 1 + m\theta$ and $\alpha_2 = 1 + m(1 - \theta)$, where $m > 0$. This parameterization not only signifies the parameter of central interest, θ , but also makes α_1 and α_2 larger than one, ensuring the existence of a unique mode. The variance of the beta distribution under this parameterization is $(1 + m\theta)\{1 + m(1 - \theta)\}/\{(2 + m)^2(3 + m)\}$, suggesting a smaller variance as m increases.

To complete the formulation of a regression model, we assume that, given \mathbf{X} , the mode of Y relates to a linear predictor $\eta(\mathbf{X}) = \beta_0 + \beta_1^T \mathbf{X}$ via a link function $g(t)$, that is,

$$\text{Mode}(Y|\mathbf{X}) = \theta(\mathbf{X}) = g\{\eta(\mathbf{X})\}. \quad (2.3)$$

Commonly employed link functions include logit, probit, log-log, and complementary log-log. To this end, we have two regression models for Y once a link function is chosen, written succinctly as

$$\begin{aligned} Y|\mathbf{X} &\sim \text{Beta}(1 + m\theta(\mathbf{X}), 1 + m\{1 - \theta(\mathbf{X})\}), \\ Y|\mathbf{X} &\sim \text{GBP}(\theta(\mathbf{X}), m), \end{aligned}$$

which are henceforth referred to as the beta mode model and the GBP mode model, respectively.

2.2 Maximum likelihood estimation

Given a random sample of size n , $\mathcal{D} = \{(Y_i, \mathbf{X}_i), i = 1, \dots, n\}$, the log-likelihood function associated with a beta mode model is

$$\begin{aligned} \ell_{\text{beta}}(\boldsymbol{\Omega}; \mathcal{D}) &= n \log \Gamma(2 + m) - \sum_{i=1}^n \log (\Gamma \{1 + m\theta(\mathbf{X}_i)\} \Gamma [1 + m \{1 - \theta(\mathbf{X}_i)\}]) \\ &\quad + m \sum_{i=1}^n [\theta(\mathbf{X}_i) \log Y_i + \{1 - \theta(\mathbf{X}_i)\} \log(1 - Y_i)]. \end{aligned}$$

Maximizing $\ell_{\text{beta}}(\boldsymbol{\Omega}; \mathcal{D})$ with respect to $\boldsymbol{\Omega} = (\boldsymbol{\beta}^T, m)^T$ yields the MLE for $\boldsymbol{\Omega}$ under this model, where $\boldsymbol{\beta} = (\beta_0, \boldsymbol{\beta}_1^T)^T$. Because the beta family is an exponential family, the corresponding likelihood function is concave, suggesting the existence of a unique MLE for $\boldsymbol{\Omega}$. Furthermore, regularity conditions required for the MLE to be consistent and asymptotically normal can also be easily verified for this regression model.

When a GBP mode model is assumed, by (2.2), the log-likelihood function is given by

$$\ell_{\text{GBP}}(\boldsymbol{\Omega}; \mathcal{D}) = n \log \left\{ \frac{(2m + 1)(m + 1)}{3m + 1} \right\} + m \sum_{i=1}^n \log d_i + \sum_{i=1}^n \log (2 - d_i^m), \quad (2.4)$$

where $d_i = I\{0 < Y_i \leq \theta(\mathbf{X}_i)\}\{Y_i/\theta(\mathbf{X}_i)\} + I\{\theta(\mathbf{X}_i) < Y_i < 1\}\{(1 - Y_i)/\{1 - \theta(\mathbf{X}_i)\}\}$.

Maximizing $\ell_{\text{GBP}}(\boldsymbol{\Omega}; \mathcal{D})$ with respect to $\boldsymbol{\Omega}$ yields the MLE for $\boldsymbol{\Omega}$ under the GBP mode regression model. Unlike the beta family, the GBP family is not an exponential family. For simplicity, let us assume m known in (2.2) and focus on the density as a function of θ for now. It can be shown that $\lim_{\theta \rightarrow v^+} (\partial^2 / \partial \theta^2) \log f_{\text{GBP}}(v; \theta, m) = -2m^2/v^2$, whereas $\lim_{\theta \rightarrow v^-} (\partial^2 / \partial \theta^2) \log f_{\text{GBP}}(v; \theta, m) = -2m^2/(1-v)^2$, indicating that the Hessian function is discontinuous at any realization of the distribution except for $v = 0.5$. It can also be shown that, the GBP log-likelihood is concave in a neighborhood of the truth almost surely. Moreover, regularity conditions (Cox and Hinkley, 1979, page 281) for the consistency of MLE as the maximizer of (2.4) are satisfied for the GBP regression model, but additional conditions needed to establish asymptotic normality for MLE are not.

3 Model diagnostics

3.1 Graphical diagnosis

Half-normal residual plots with simulated envelopes (Atkinson, 1987) are useful graphical tools for checking the goodness-of-fit of a model with complex response distributions. Let $\hat{\mu}(\mathbf{x})$ and $\hat{\sigma}^2(\mathbf{x})$ denote the MLEs for the mean and variance of Y given $\mathbf{X} = \mathbf{x}$, respectively, resulting from an assumed regression model. Define the absolute standardized residual as $r_i = |Y_i - \hat{\mu}(\mathbf{X}_i)| / \hat{\sigma}(\mathbf{X}_i)$. Given data $\mathcal{D} = \{(Y_i, \mathbf{X}_i), i = 1, \dots, n\}$, the algorithm below describes how to obtain a half-normal residual plot with a simulated envelope.

Step 1: Fit the assumed regression model to data \mathcal{D} , calculate the absolute standardized residuals, then order the residuals from smallest to largest, denoted as $\{r_{(i)}, i = 1, \dots, n\}$. Plot $r_{(i)}$ against the half-normal quantile $q_i = \Phi^{-1}\{(i+n-0.125)/(2n+0.5)\}$, for $i = 1, \dots, n$, where $\Phi(\cdot)$ is the cumulative distribution function of $N(0, 1)$.

Step 2: For $k = 1, \dots, 19$, conditioning on \mathbf{X}_i , generate a new response $Y_i^{*(k)}$ from the estimated regression model resulting from *Step 1*, for $i = 1, \dots, n$. This produces new

data $\mathcal{D}^{*(k)} = \{(Y_i^{*(k)}, \mathbf{X}_i), i = 1, \dots, n\}$, for $k = 1, \dots, 19$.

Step 3: For $k = 1, \dots, 19$, fit the assumed regression model to data $\mathcal{D}^{*(k)}$ and calculate the ordered absolute standardized residuals $\{r_{(i)}^{*(k)}, i = 1, \dots, n\}$.

Step 4: Compute $r_i^L = \min_{1 \leq k \leq 19} \{r_{(i)}^{*(k)}\}$ and $r_i^U = \max_{1 \leq k \leq 19} \{r_{(i)}^{*(k)}\}$, for $i = 1, \dots, n$. Plot points $\{(x, y) : (q_i, r_i^L), i = 1, \dots, n\}$ and $\{(x, y) : (q_i, r_i^U), i = 1, \dots, n\}$ on the same plot obtained in *Step 1* to form the envelope.

If the assumed model agrees with the true model, the ordered residuals $r_{(i)}$ obtained from the original data are expected to lie inside the envelope with probability approximately equal to 0.95 (Atkinson, 1987). A substantially larger proportion of residuals falling outside the envelope indicates a lack-of-fit of the assumed model.

3.2 Score tests for model diagnosis

To assess the adequacy of an assumed regression model quantitatively, we develop tests using score functions constructed based on matching moments. The proposed score tests exploit certain moments of the response variable or functions of it that are special in some way so that they are difficult to be estimated well via maximizing a misspecified likelihood function.

When the assumed model is a beta mode model, we construct a bivariate score function based on the following results relating to a beta random variable V ,

$$E(\log V) = \psi(\alpha_1) - \psi(\alpha_1 + \alpha_2),$$

$$E(V \log V) = \frac{\alpha_1 \{\psi(\alpha_1 + 1) - \psi(\alpha_1 + \alpha_2 + 1)\}}{\alpha_1 + \alpha_2},$$

where $\psi(t) = \{(d/dt)\Gamma(t)\}/\Gamma(t)$ is the digamma function. Matching these two expectations with their sample counterparts, we formulate the following score function evaluated at

(Y_i, \mathbf{X}_i) for model diagnosis when the assumed regression model is a beta mode model,

$$\mathbf{S}_{i,\text{beta}}(\boldsymbol{\Omega}) = \left[\begin{array}{c} \log Y_i - \psi\{1 + m\theta(\mathbf{X}_i)\} + \psi(2 + m) \\ Y_i \log(Y_i) - \frac{\{1 + m\theta(\mathbf{X}_i)\} [\psi\{2 + m\theta(\mathbf{X}_i)\} - \psi(3 + m)]}{2 + m} \end{array} \right]. \quad (3.1)$$

If the assumed model is a GBP mode model, we formulate a bivariate score function based on matching the first two moments of $Y|\mathbf{X} \sim \text{GBP}(\theta(\mathbf{X}), m)$ (García et al., 2009),

$$\begin{aligned} E(Y|\mathbf{X}) &= \frac{6m^2\theta(\mathbf{X}) + 7m + 2}{6m^2 + 14m + 4}, \\ \text{Var}(Y|\mathbf{X}) &= \{4(3m + 1)^2(m + 2)^2(2m + 3)(m + 3)\}^{-1} [4m^2(37m^2 + 61m \\ &\quad + 10)\theta(\mathbf{X})\{\theta(\mathbf{X}) - 1\} + 82m^4 + 247m^3 + 247m^2 + 96m + 12]. \end{aligned}$$

That is, the score function evaluated at (Y_i, \mathbf{X}_i) for assessing the adequacy of an assumed GBP mode model is

$$\mathbf{S}_{i,\text{GBP}}(\boldsymbol{\Omega}) = \left[\begin{array}{c} Y_i - E(Y_i|\mathbf{X}_i) \\ Y_i^2 - \text{Var}(Y_i|\mathbf{X}_i) - \{E(Y_i|\mathbf{X}_i)\}^2 \end{array} \right]. \quad (3.2)$$

Generically denote by $\mathbf{S}_i(\boldsymbol{\Omega})$ the score function in (3.1) or (3.2), depending on whether one assumes a beta mode model or a GBP mode model. We mimic the Hotelling's T^2 statistic (Hotelling, 1931) to define the following test statistic,

$$Q(\hat{\boldsymbol{\Omega}}; \mathcal{D}) = \frac{n - 2}{2(n - 1)} \bar{\mathbf{S}}^T \hat{\boldsymbol{\Sigma}}^{-1} \bar{\mathbf{S}}, \quad (3.3)$$

where $\hat{\boldsymbol{\Omega}}$ is the MLE of $\boldsymbol{\Omega}$ under the assumed model, $\bar{\mathbf{S}} = n^{-1} \sum_{i=1}^n \mathbf{S}_i(\hat{\boldsymbol{\Omega}})$, and $\hat{\boldsymbol{\Sigma}} = \{n(n - 1)\}^{-1} \sum_{i=1}^n \{\mathbf{S}_i(\hat{\boldsymbol{\Omega}}) - \bar{\mathbf{S}}\} \{\mathbf{S}_i(\hat{\boldsymbol{\Omega}}) - \bar{\mathbf{S}}\}^T$ is an estimator for the variance-covariance of $\bar{\mathbf{S}}$. Under the null hypothesis that the assumed model is the true model, one has $E(\bar{\mathbf{S}}) = \mathbf{0}$ when evaluating $\hat{\boldsymbol{\Omega}}$ at the truth, and thus a small value for $Q(\hat{\boldsymbol{\Omega}}; \mathcal{D})$ is expected under the null. In contrast, when the assumed model differs from the true model to the extent that $E(\bar{\mathbf{S}})$

substantially deviates from zero, a large realization of $Q(\hat{\Omega}; \mathcal{D})$ is expected. According to Hotelling (1931), if $\mathbf{S}_i(\Omega)$ is a bivariate normal random variable, then $Q(\Omega; \mathcal{D}) \sim F_{2, n-2}$ under the null. With a response supported on $[0, 1]$, a bivariate normal is not likely to approximate well the distributions of the scores in (3.1) and (3.2), although a large $Q(\hat{\Omega}; \mathcal{D})$ still implies poor fit for relevant moments and thus casts doubt on the assumed model. To accurately approximate certain percentiles of the null distribution of $Q(\hat{\Omega}; \mathcal{D})$, we use a parametric bootstrap procedure that leads to an estimated p -value associated with the test statistic. The algorithm in supplementary Section S1 outlines the bootstrap procedure under the null stating that the true model is a GBP mode model. A similar bootstrap procedure is used to estimate the p -value of the test statistic when one assumes a beta mode model.

Empirical evidence from simulation studies suggest that this bootstrap procedure can estimate the tail of the null distribution of $Q(\hat{\Omega}; \mathcal{D})$ well enough to preserve the right size of the proposed score tests. Besides how well one can estimate certain percentiles of a null distribution, operating characteristics of the score tests also depend on the extent of distortion on moment estimation when an inadequate model is assumed. More empirical evidence on this aspect are presented next, along with the performance of maximum likelihood estimation and predictions based on synthetic data generated from various regression models.

4 Simulation study

4.1 Design of simulation experiments

In all experiments, we simulate a bivariate covariate, $\mathbf{X} = (X_1, X_2)^T$, as the predictor in a regression model. When carrying out regression analysis, we assume a linear predictor, $\eta(\mathbf{X}) = \beta_0 + \beta_1 X_1 + \beta_2 X_2$, and the logit link $g(t) = 1/(1 + e^{-t})$ in (2.3), despite the true data generating process.

When conducting regression analysis assuming a beta mode model, we first simulate X_2 from Bernoulli(0.5), and then generate data for X_1 according to $N(I(X_2 = 1) - I(X_2 = 0), 1)$.

Given covariates data, responses are generated from each of the following four conditional distributions:

$$(B1) Y|\mathbf{X} \sim \text{Beta}(1 + m\theta(\mathbf{X}), 1 + m\{1 - \theta(\mathbf{X})\}), \text{ where } \theta(\mathbf{X}) = 1/[1 + \exp\{-\eta(\mathbf{X})\}], \text{ with } \eta(\mathbf{X}) = 1 + X_1 + X_2;$$

$$(B2) Y|\mathbf{X} \sim \text{Beta}(1 + m\theta(\mathbf{X}), 1 + m\{1 - \theta(\mathbf{X})\}), \text{ where } \theta(\mathbf{X}) = 1/[1 + \exp\{-\eta(\mathbf{X})\}], \text{ with } \eta(\mathbf{X}) = 1 + X_1 + X_1^2 + X_2;$$

$$(B3) Y|\mathbf{X} \sim \text{Beta}(1 + m\theta(\mathbf{X}), 1 + m\{1 - \theta(\mathbf{X})\}), \text{ where } \theta(\mathbf{X}) = 0.5\Phi[2\{\eta(\mathbf{X}) + 2\}] + 0.5\Phi[2\{\eta(\mathbf{X}) - 2\}], \text{ with } \eta(\mathbf{X}) = 1 + X_1 + X_2;$$

$$(B4) Y|\mathbf{X} \sim \text{GBP}(\theta(\mathbf{X}), m), \text{ where } \theta(\mathbf{X}) = 1/[1 + \exp\{-\eta(\mathbf{X})\}], \text{ with } \eta(\mathbf{X}) = 1 + X_1 + X_2.$$

When a GBP mode model is assumed for regression analysis, we consider the following four regression models according to which responses are generated after data for X_1 are simulated from $N(0, 1)$ and data for X_2 are simulated from Bernoulli(0.5):

$$(G1) Y|\mathbf{X} \sim \text{GBP}(\theta(\mathbf{X}), m), \text{ where } \theta(\mathbf{X}) = 1/[1 + \exp\{-\eta(\mathbf{X})\}], \text{ with } \eta(\mathbf{X}) = 1 + X_1 + X_2;$$

$$(G2) Y|\mathbf{X} \sim \text{GBP}(\theta(\mathbf{X}), m), \text{ where } \theta(\mathbf{X}) = 1/[1 + \exp\{-\eta(\mathbf{X})\}], \text{ with } \eta(\mathbf{X}) = 1 + X_1 + X_1^2 + X_2;$$

$$(G3) Y|\mathbf{X} \sim \text{GBP}(\theta(\mathbf{X}), m), \text{ where } \theta(\mathbf{X}) = 0.5\Phi[2\{\eta(\mathbf{X}) + 2\}] + 0.5\Phi[2\{\eta(\mathbf{X}) - 2\}], \text{ in which } \eta(\mathbf{X}) = 1 + X_1 + X_2;$$

$$(G4) Y|\mathbf{X} \sim \text{Beta}(1 + m\theta(\mathbf{X}), 1 + m\{1 - \theta(\mathbf{X})\}), \text{ where } \theta(\mathbf{X}) = 1/[1 + \exp\{-\eta(\mathbf{X})\}], \text{ with } \eta(\mathbf{X}) = 1 + X_1 + X_2.$$

Cases (B1) and (G1) create scenarios where the assumed model coincides with the true model, and the other cases give rise to scenarios where we implement maximum likelihood estimation under a misspecified model. Under (B2) and (G2), the assumed models misspecify the linear predictor; under (B3) and (G3), the assumed models involve a misspecified link

function for the mode; and under (B4) and (G4), the assumed conditional distribution of Y given covariates is not from the same family that the true conditional distribution belongs to.

4.2 Covariates effects estimation

Given each of the above data generating processes, we generate data sets $\{(Y_i, X_{1i}, X_{2i})\}_{i=1}^n$ with $n = 50, 100$. Under each simulation setting, we repeat maximum likelihood estimation using 300 Monte Carlo data sets.

When the assumed model matches the true model, the MLE for Ω is expected to be consistent estimator. Table 1 provides summary statistics for these MLEs and the estimated standard deviations associated with these estimates based on data generated according to (B1) with $m = 80$ and (G1) with $m = 10$, where the estimated standard deviations result from sandwich variance estimation for M-estimators (Boos and Stefanski, 2013, Section 7.2.1). The close agreement between the MLE of Ω and the truth, and the resemblance between the estimated standard deviations and the empirical standard deviations suggest that the first two moments of the asymptotic distribution of the MLEs are estimated reasonably well.

4.3 Performance of model diagnosis methods

Besides covariate effects estimation, we also monitor operating characteristics of the model diagnostics tools proposed in Section 3. Assuming a beta mode model, Figure 3 demonstrates the half-normal residual plots obtained based on one data set of size $n = 100$ generated from each of (B1)–(B4), where $m = 80$ in (B1)–(B3), and $m = 10$ in (B4). Under (B1), where the assumed model matches the true data generating process, very few residuals fall outside of the envelope. In contrast, a large proportion of the residuals are outside of the envelope under (B3), where the link function is misspecified. The plot under (B2) also witnesses a rather high proportion of residuals outside of the envelope, but relatively lower proportion under (B4).

Table 1: Averages of MLEs for parameters in a beta mode model and a GBP mode model across 300 Monte Carlo replicates generated according to (B1) and (G1), respectively, and averages of the corresponding estimated standard deviations ($\widehat{\text{s.d.}}$) in comparison with the empirical standard deviations (s.d.). Numbers in parentheses are $100 \times$ (Monte Carlo standard errors) associated with the averages. The true parameter values are $\beta = (\beta_0, \beta_1, \beta_2)^T = (1, 1, 1)^T$, and $\log m = \log 80 \approx 4.382$ under (B1), $\log m = \log 10 \approx 2.303$ under (G1).

	MLE	$\widehat{\text{s.d.}}$	s.d.	MLE	$\widehat{\text{s.d.}}$	s.d.
(B1)	$n = 50$			$n = 100$		
β_0	1.000 (0.41)	0.070 (0.09)	0.071	0.996 (0.28)	0.050 (0.04)	0.049
β_1	1.000 (0.30)	0.051 (0.07)	0.052	0.997 (0.21)	0.037 (0.03)	0.036
β_2	0.991 (0.76)	0.119 (0.16)	0.131	0.997 (0.51)	0.086 (0.08)	0.089
$\log m$	4.441 (0.88)	0.130 (0.57)	0.152	4.422 (0.74)	0.120 (0.30)	0.128
(G1)	$n = 50$			$n = 100$		
β_0	0.996 (0.41)	0.078 (0.26)	0.072	0.999 (0.31)	0.053 (0.13)	0.053
β_1	0.990 (0.44)	0.076 (0.30)	0.077	0.992 (0.29)	0.048 (0.15)	0.050
β_2	0.997 (0.66)	0.123 (0.35)	0.115	0.986 (0.53)	0.086 (0.20)	0.091
$\log m$	2.362 (0.84)	0.144 (0.12)	0.145	2.325 (0.56)	0.101 (0.06)	0.097

These empirical evidence indicate that the half-normal residual plot is an effective graphical indicator of link misspecification and linear predictor misspecification. The relatively weaker indication of lack-of-fit when the truth is a GBP mode model suggests that assuming a beta mode model for data from GBP models may not drastically compromise inference for the first two moments.

Assuming a GBP mode model, Figure 4 demonstrates the half-normal residual plots using one data set of size $n = 100$ generated from each of (G1)–(G4), where $m = 10$ in (G1)–(G3), and $m = 80$ in (G4). Similar to what one sees in the previous figure, in the absence of model misspecification as in (G1), most residuals are within the envelope. A much larger proportion of residuals fall outside of the envelope in the presence of link misspecification as in (G3). The plots also exhibit a moderate to high proportion of residuals outside of the envelopes under (G2) and (G4). Hence, the effectiveness of the half-normal residual plot for detecting various sources of model misspecification is also evident when one assumes a GBP mode model.

Figure 5 presents the empirical power of the score tests proposed in Section 3.2 when a beta mode model or a GBP mode model is assumed, where the empirical power of a

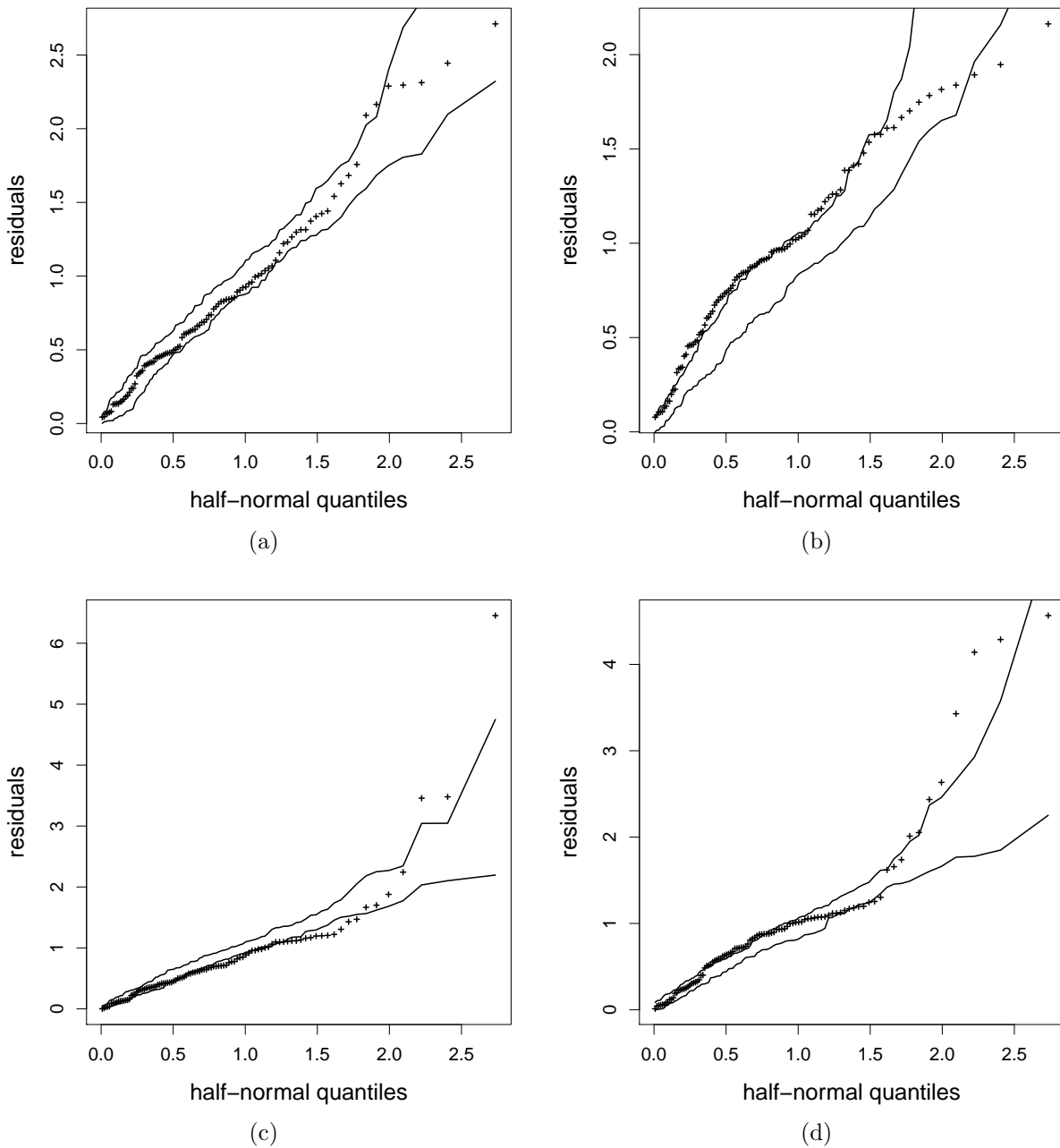
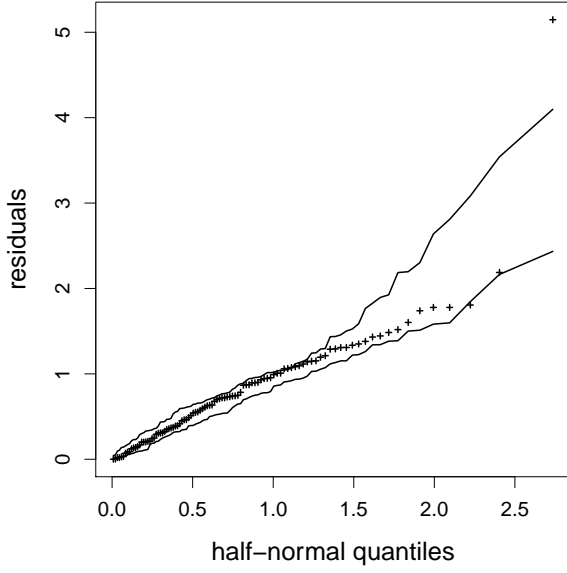
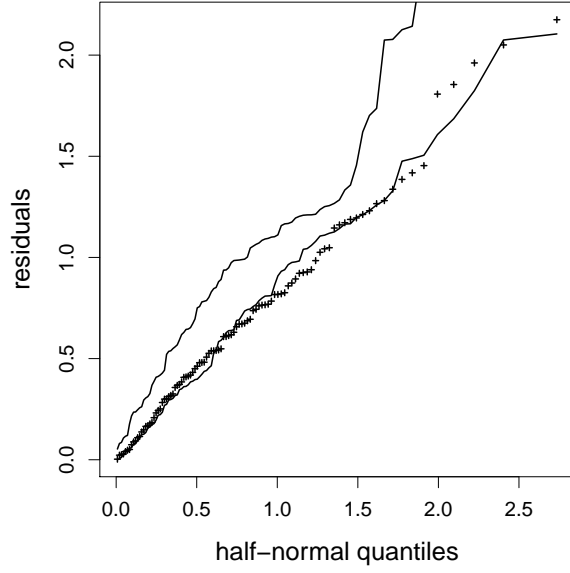


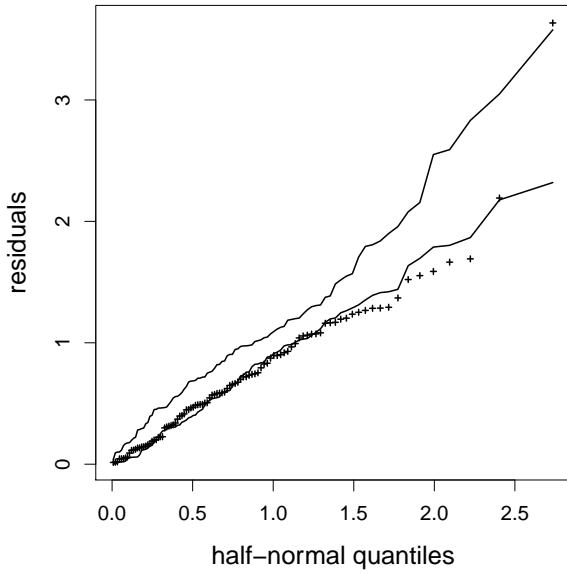
Figure 3: Half-normal residual plots with simulated envelopes based on one random sample of size $n = 100$ when one assumes a beta mode model for data generated from (B1)–(B4), shown in (a)–(d), respectively.



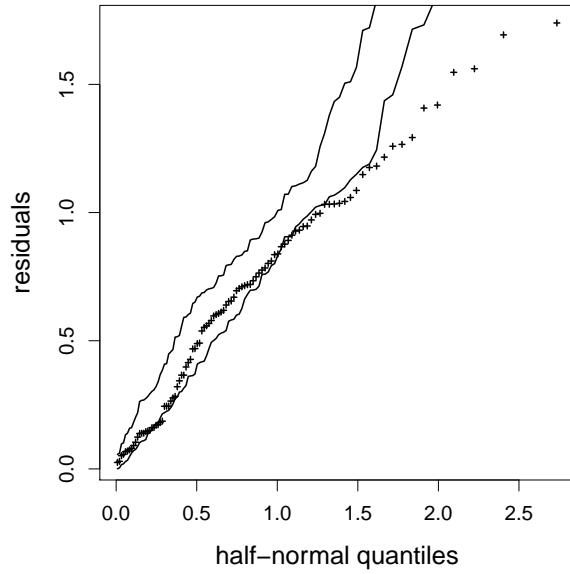
(a)



(b)



(c)



(d)

Figure 4: Half-normal residual plots with simulated envelopes based on one random sample of size $n = 100$ when one assumes a GBP mode model for data generated from (G1)–(G4), shown in (a)–(d), respectively.

test is defined as the rejection rate of the test at significance level 0.05 across 300 Monte Carlo replicates under each true model specification. Given one simulated data set, we use 300 bootstrap samples to estimate the p -value associated with a score test. These empirical power indicate that the size of the score tests remain close to the nominal level in the absence of model misspecification, and, as the sample size grows, their power to detect any one of the three sources of model misspecification increases. Under each assumed mode model, the proposed score test has the highest power to detect a link misspecification, moderate power in response to a misspecified linear predictor, and the lowest power when the conditional distribution family is misspecified. The low power to detect the last type of model misspecification, especially when a beta mode model is assumed, may suggest that, given a GBP mode model, there exists a member in the family of beta mode models that can approximate the GBP mode model well enough to produce reasonable estimates for the first two moments. Lastly, these numerical evidence of model misspecification match nicely with the graphical evidence from half-normal residual plots in that a higher rejection rate observed for the score test under one scenario usually goes with a higher proportion of residuals outside of the envelope in the half-normal residual plot in the same scenario.

4.4 Predictions

Predicting an outcome is often one of the ultimate goals in regression analysis, such as in ADNI where accurate prediction of AD progression is a major goal. Suppose \mathbf{x} is the covariate value at which one wishes to predict a bounded outcome, such as one's ADAS-11 score. In what follows, at a nominal coverage probability $q \in (0, 1)$, we first construct a prediction interval based on an estimated mode, denoted by $\mathcal{PI}_\theta(\mathbf{x}, q)$, then we formulate a prediction interval based on an estimated mean, denoted by $\mathcal{PI}_\mu(\mathbf{x}, q)$. Define $e = Y - \theta(\mathbf{x})$ as the mode residual, and denote by $f_e(e|\mathbf{x})$ the pdf of e given $\mathbf{X} = \mathbf{x}$.

Under an assumed mode regression model, following maximum likelihood estimation of $\boldsymbol{\Omega}$, one obtains the MLEs for $\theta(\mathbf{x})$ and $\mu(\mathbf{x})$, as well as an estimated pdf of e given $\mathbf{X} = \mathbf{x}$.

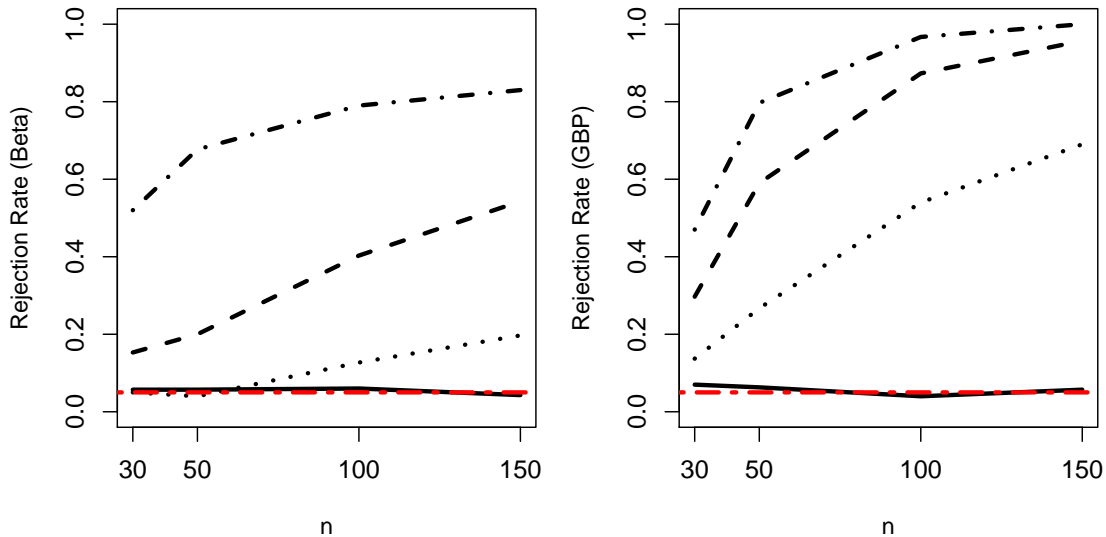


Figure 5: Rejection rates across 300 Monte Carlo replicates associated with the score tests under (B1)–(B4) when a beta mode model is assumed (in the left panel), and under (G1)–(G4) when a GBP mode model is assumed (in the right panel). True model settings are: solid lines for (B1)&(G1), dashed lines for (B2)&(G2), dashed-dotted lines for (B3)&(G3), and dotted lines for (B4)&(G4). Red horizontal two-dashed lines are reference lines at nominal level 0.05.

Denote these MLEs by $\hat{\theta}(\mathbf{x})$ and $\hat{\mu}(\mathbf{x})$, respectively, and denote by $\hat{f}_e(e|\mathbf{x})$ the estimated pdf. Then, based on these estimates, the narrowest $\mathcal{PI}_\theta(\mathbf{x}, q)$ is $[\hat{\theta}(\mathbf{x}) + e_1, \hat{\theta}(\mathbf{x}) + e_2]$, where $e_1 < 0 < e_2$ satisfy $\hat{f}_e(e_1|\mathbf{x}) = \hat{f}_e(e_2|\mathbf{x})$ and $\int_{e_1}^{e_2} \hat{f}_e(e|\mathbf{x}) de = q$.

To formulate a $(100 \times q)\%$ mean-based prediction interval, we first make sure that $\hat{\mu}(\mathbf{x}) \in \mathcal{PI}_\mu(\mathbf{x}, q)$, then we construct an interval with the desired coverage probability that is close to $\hat{\theta}(\mathbf{x})$ as much as possible in order to achieve the narrowest $\mathcal{PI}_\mu(\mathbf{x}, q)$. Clearly, if $\hat{\mu}(\mathbf{x})$ already falls in $\mathcal{PI}_\theta(\mathbf{x}, q)$ constructed above, which is the narrowest by construction, then one may also use this interval as $\mathcal{PI}_\mu(\mathbf{x}, q)$. Otherwise, we construct $\mathcal{PI}_\mu(\mathbf{x}, q)$ with $\hat{\mu}(\mathbf{x})$ on one of the boundaries depending on how $\hat{\mu}(\mathbf{x})$ compares with $\hat{\theta}(\mathbf{x})$. In particular, if $\hat{\mu}(\mathbf{x}) \geq \hat{\theta}(\mathbf{x})$, then we set $\mathcal{PI}_\mu(\mathbf{x}, q) = [\hat{\mu}(\mathbf{x}) - c, \hat{\mu}(\mathbf{x})]$, where $c > 0$ is chosen such that $\int_{\hat{\mu}(\mathbf{x}) - c}^{\hat{\mu}(\mathbf{x})} \hat{f}_{Y|\mathbf{X}}(y|\mathbf{x}) dy = q$, in which $\hat{f}_{Y|\mathbf{X}}(y|\mathbf{x})$ is pdf of the assumed distribution of Y given $\mathbf{X} = \mathbf{x}$ evaluated at $\hat{\Omega}$. If $\hat{\mu}(\mathbf{x}) < \hat{\theta}(\mathbf{x})$, then we let $\mathcal{PI}_\mu(\mathbf{x}, q) = [\hat{\mu}(\mathbf{x}), \hat{\mu}(\mathbf{x}) + c]$, where $c > 0$ satisfies $\int_{\hat{\mu}(\mathbf{x})}^{\hat{\mu}(\mathbf{x}) + c} \hat{f}_{Y|\mathbf{X}}(y|\mathbf{x}) dy = q$.

With the assumed model being a GBP mode model, Figure 6 depicts in upper panels averages empirical coverage probabilities of $\mathcal{PI}_\theta(\cdot, q)$ and $\mathcal{PI}_\mu(\cdot, q)$ versus nominal coverage probabilities q when 300 Monte Carlo replicate data sets are generated from (G1) with $m = 10$ and $n = 50, 150$, where q ranges from 0.05 to 0.5. The empirical coverage probability of each type of prediction intervals is obtained via leave-one-out cross validation. Take $\mathcal{PI}_\theta(\cdot, q)$ as an example, its empirical coverage probability based on one data set is defined as $n^{-1} \sum_{i=1}^n I\{Y_i \in \mathcal{PI}_\theta^{(-i)}(\mathbf{X}_i, q)\}$, where $\mathcal{PI}_\theta^{(-i)}(\mathbf{X}_i, q)$ is the $(100 \times q)\%$ mode-based prediction interval constructed using data $\mathcal{D}_{-i} = \{(Y_j, \mathbf{X}_j), j = 1, \dots, n, j \neq i\}$. The lower panels of Figure 6 compare the average width of $\mathcal{PI}_\theta(\cdot, q)$ with that of $\mathcal{PI}_\mu(\cdot, q)$. Parallel pictures when data are generated from (B1) with $m = 10$ and one assumes a beta mode model are provided in supplementary Figure S1.

According to these figures, mode-based prediction intervals and mean-based prediction intervals achieve similar empirical coverage probabilities that become closer to the nominal coverage probability as n increases. More importantly, the mode-based prediction interval tends to be narrower than the mean-based prediction interval. By construction, it is expected that $\mathcal{PI}_\theta(\mathbf{x}, q) = \mathcal{PI}_\mu(\mathbf{x}, q)$ when q is not low since $\mathcal{PI}_\theta(\mathbf{x}, q)$ with a moderate or high coverage probability is very likely to include the estimated mean.

5 Regression analysis in two applications

We entertain in this section two data sets from real life applications where a bounded response is of interest. Besides carrying out mode regression analysis to infer the association between the response and some potentially influential covariates identified by previous studies, we also adopt the beta mean regression model for a rate or proportion response proposed by Ferrari and Cribari-Neto (2004) to study the association. In their proposed regression model, the authors reparameterized the beta distribution by setting $\alpha_1 = \mu\phi$ and $\alpha_2 = (1 - \mu)\phi$, where $\mu \in [0, 1]$ is the mean parameter and ϕ is a positive shape parameter, with a larger

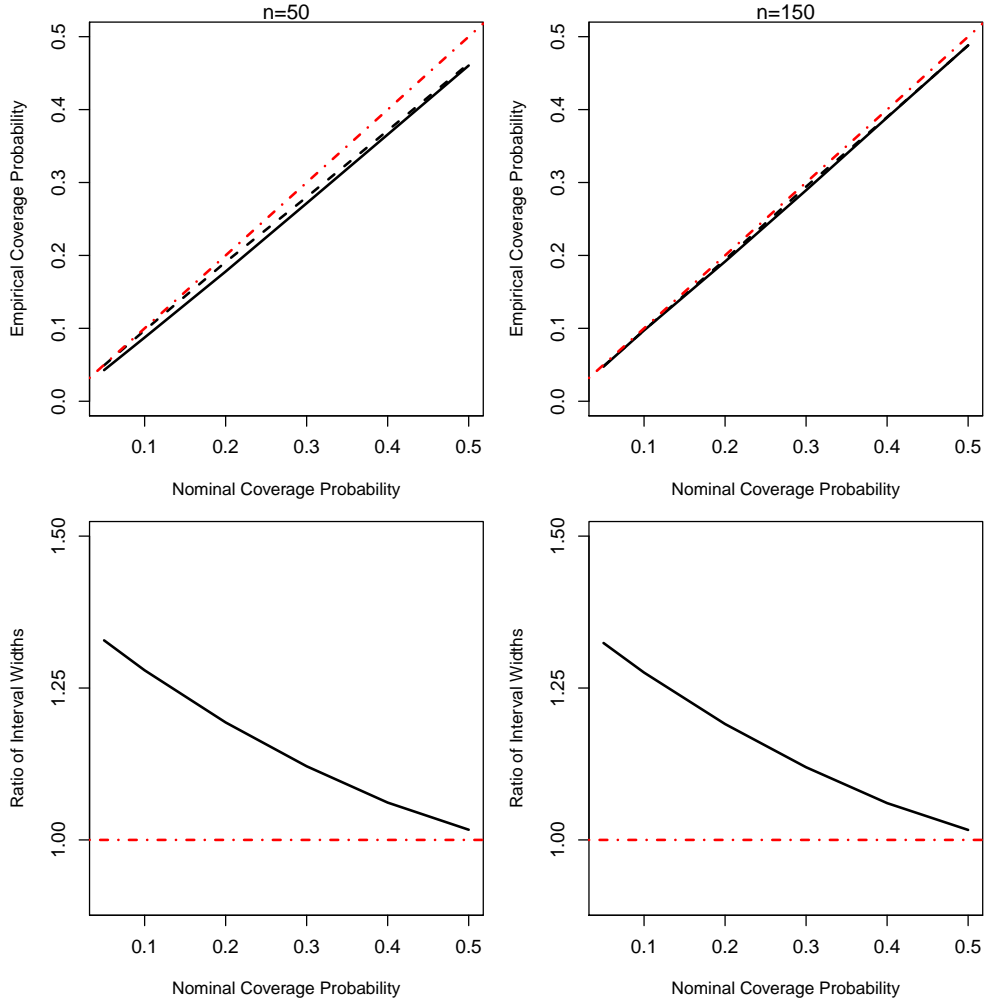


Figure 6: Prediction intervals based on data from the GBP mode model in (G1) with $m = 10$. Top panels depict average empirical coverage probabilities (across 300 Monte Carlo replicates) of mode-based prediction intervals (solid lines), and those of mean-based prediction intervals (dashed lines) versus nominal coverage probabilities. Red dash-dotted lines are 45° reference lines. Lower panels depict ratios of the average width of mean-based prediction intervals over that of mode-based prediction intervals versus nominal coverage probabilities (solid lines). Red dash-dotted horizontal lines are reference lines at value one.

ϕ resulting in a smaller variance, and they incorporated the linear predictor $\eta(\mathbf{X})$ by letting $\mu = g\{\eta(\mathbf{X})\}$.

5.1 ADNI data

There has been a consensus among medical researchers that regional brain atrophy in the medial temporal lobe structures, such as the entorhinal cortex (ERC) and hippocampus (HPC), are correlated with clinical alterations in the pre-dementia phase of mild cognitive impairment (MCI) and various dementia phases of AD (Devanand et al., 2007; Jauhiainen et al., 2009). While early detection and intervention in MCI subjects has been actively pursued by many researchers, there are mixed opinions among researchers regarding the roles volumetric measures of ERC and HPC play in predicting an MCI subject’s risk of developing AD (Jack et al., 1999; Killiany et al., 2002; deToledo Morrell et al., 2004; Hämäläinen et al., 2007; Whitwell et al., 2008).

Here, we apply the proposed mode regression models and the aforementioned mean regression model to data from the ADNI database (adni.loni.usc.edu) to study the association between one’s ADAS-11 score at month 12 and the volumetric changes in ERC and HPC at month 6 compared to their baseline measures. In particular, the dataset we consider consists of a cohort of 245 subjects who was diagnosed with LMCI when they entered the ADNI Phase 1 study and were followed up at least at both months 6 and 12. The original response variable is a subject’s ADAS-11 score at month 12, which has a bounded support on $[0, 70]$. We rescale the support to the unit interval by dividing ADAS-11 scores by 70. In a preliminary analysis, we fit the beta mean model, beta mode model, and GBP mode model to the data using various link functions $g(t)$. Table 2 reports values of log-likelihood function resulting from these assumed models with three choices of $g(t)$ (see the left half of the table). Observing the highest value of log-likelihood when $g(t)$ is the log-log link across all three regression models, we use the log-log link in the regression models for further analysis.

Panels (a) and (b) in Figure 7 provide the half-normal residual plots associated with the

Table 2: Values of log-likelihood under each regression model using three link functions for the ADNI data and for the compositional data

Model	logit	log-log	probit	logit	log-log	probit
	ADNI data			Compositional data		
beta mean model	260.99	261.10	261.03	117.34	118.39	117.62
beta mode model	260.86	261.00	260.92	117.25	118.50	117.58
GBP mode model	238.10	238.16	238.13	121.58	124.33	121.99

beta mode model and GBP mode model based on this data set. Having majority of the residuals from GBP mode regression falling outside of the envelope suggests a poor fit of the GBP model for the data, and the beta mode model is more adequate for the current data. The score test when the null hypothesis states a beta mode model yields an estimated p -value of 0.44, while the score test when one assumes a GBP mode model gives an estimated p -value of 0. Gathering these graphical and numerical diagnosis, we conclude that the beta mode model potentially captures the underlying conditional distribution better than the GBP mode model does.

Table 3 provides MLEs of unknown parameters in each of the three considered regression models. According to Table 3, inference for the covariate effects from all three regression models suggest that the volumetric change in ERC is a statistically significant predictor for one’s cognitive impairment. However, results from the GBP mode model does not indicate that the volumetric change in HPC is significantly associated with the response (with a p -value of 0.304), although inference from both beta mode and beta mean model imply a significant effect of the change in hippocampal volume on the ADAS-11 score (with p -values 0.045 and 0.042, respectively). The differences between the estimated regression coefficients based on the beta mean model and those from the beta mode model suggest that the underlying conditional distribution of the response may be skewed, leading to different covariate effects manifested via the conditional mean and mode. Although relating to the marginal distribution as opposed to the conditional distribution of the response, the histogram of ADAS-11 scores in Figure 1 may suggest that the conditional distribution of

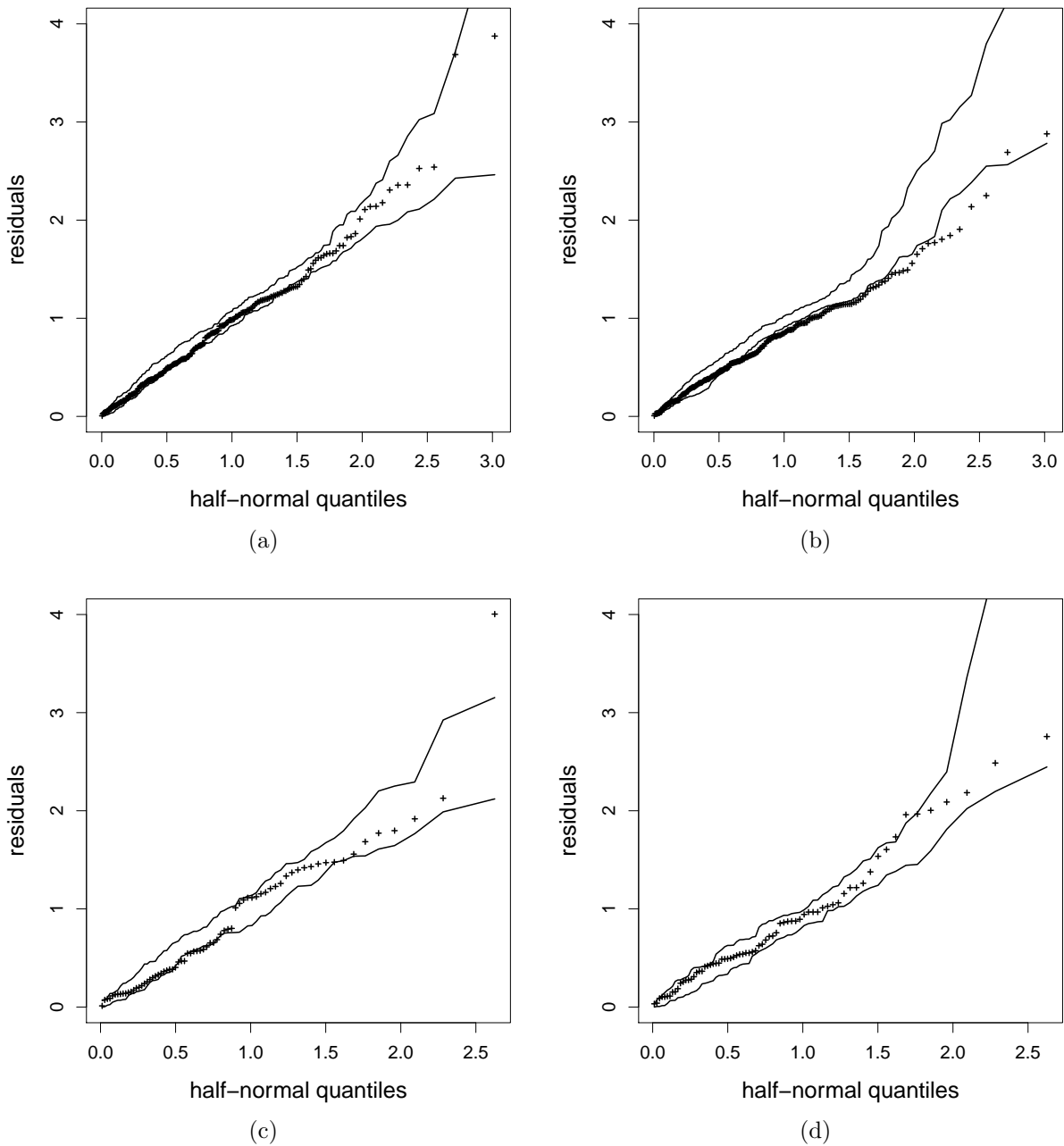


Figure 7: Half-normal residual plots with simulated envelope for the ADNI data associated with the beta mode model (in (a)) and the GBP mode model (in (b)), and corresponding plots for the compositional data in (c) and (d).

Table 3: Maximum likelihood estimates corresponding to each regression model for the ADNI data. Numbers in parentheses are estimated standard errors associated with the MLEs.

Parameter	Beta mean model	Beta mode model	GBP mode model
β_0 (Intercept)	-0.552 (0.020)	-0.692 (0.026)	-0.964 (0.018)
β_1 (ERC.change)	-0.102 (0.043)	-0.124 (0.052)	-0.116 (0.029)
β_2 (HPC.change)	-0.170 (0.083)	-0.215 (0.107)	-0.116 (0.113)
ϕ or $\log m$	18.061 (1.615)	2.777 (0.101)	1.826 (0.068)

Table 4: Five-fold cross-validated coverage probabilities of mode-based prediction intervals, $\mathcal{PI}_\theta(\cdot, q)$, and mean-based prediction intervals, $\mathcal{PI}_\mu(\cdot, q)$, under each regression model for the ADNI data. Nnumbers in parentheses are the average widths of the prediction intervals.

q	Beta mode model		GBP mode model	
	\mathcal{PI}_θ	\mathcal{PI}_μ	\mathcal{PI}_θ	\mathcal{PI}_μ
0.1	0.131 (0.021)	0.082 (0.022)	0.090 (0.020)	0.098 (0.028)
0.2	0.229 (0.043)	0.192 (0.044)	0.167 (0.041)	0.253 (0.053)
0.5	0.547 (0.114)	0.547 (0.114)	0.518 (0.114)	0.531 (0.117)

the response is indeed skewed.

We next construct prediction intervals based on the estimated densities from beta mode regression and GBP mode regression following the method described in Section 4.4. For each regression model, we compare the mode-based prediction interval and the mean-based prediction interval, $\mathcal{PI}_\theta(\cdot, q)$ and $\mathcal{PI}_\mu(\cdot, q)$, for a given q in regard to their empirical coverage probabilities and widths. A five-fold cross validation procedure is used to obtain the empirical coverage probability of a considered type of prediction interval. Between the two types of prediction intervals based on different central tendency measures, the narrower interval that also has an empirical coverage probability close to q is more preferable. Table 4 reports summary statistics of these prediction intervals. Comparing the mode-based prediction interval and the mean-based prediction interval with a fixed q under each mode regression model, one can see that the former tends to be narrower than the latter when q is small, while both possessing empirical coverage probabilities close to the nominal level. Hence, in this application of assessing an LMCI subject's extent of cognitive impairment in the near future, using the mode tends to provide more accurate prediction than when using the mean.

5.2 Compositional data

In a geological study of the composition of sediment generated from the drainage basin in Blue Ridge Mountains, Grantham and Velbel (1988) compiled data of $n = 72$ sediment samples to record proportions of four petrographic types of sediment grains and certain characteristics of the drainage basin. For illustration purposes, we use the proportion of grains of one single quartz crystal as the response. As in the analysis of the same data presented in Van den Boogaart and Tolosana-Delgado (2013, Section 5.3), the following four explanatory variables are included in our regression analysis: a dichotomous variable describing the position of the river (either northern or southern part of the drainage basin), the river discharge as a measure of outflowing annual volume of water per area of the drainage area above the measurement location, the relief as the slope of the river trace, and a tripartite variable referred to as grain, which indicates the size of sediment grains, including three levels, fine, median, and coarse. For the two categorical variables, which are position and grain, one dummy variable, position-s (for southern), is created for the former, and two dummy variables are created for the latter, grain-f and grain-m, relating to the first two levels of grain size.

Under each of the beta mean model, beta mode model, and GBP mode model, the log-log link yields the highest log-likelihood function among the three considered link functions (see the right half of Table 2). Panels (c) and (d) in Figure 7 provide the half-normal residual plots associated with the beta mode model and GBP mode model based on this data set. It appears that more residuals stay inside the envelope when the GBP mode model is assumed, with only two residuals outside of the envelope yet are very close to the upper bound of it, whereas there are more residuals outside of the envelope under the beta mode model, with one far beyond the envelope region. The score test when the null hypothesis states a GBP mode model yields an estimated p -value of 0.57, while the score test when one assumes a beta mode model gives an estimated p -value of 0.08. Gathering these graphical and numerical evidence, we conclude that the GBP mode model potentially captures the underlying conditional

distribution better than the beta mode model does, although both models may not reflect certain features of the truth, such as possibly multimodality according to the histogram of the response in supplementary Figure S2. Supplementary Table S1 provides the MLEs for parameters in these regression models. The inference from the GBP mode model implies a more significant effect of the grain size than the same covariate effect inferred by the possibly misspecified beta mean model or the beta mode model.

Due to the small sample size and potential model misspecification, constructing prediction intervals based on a parametrically estimated density as described in Section 4.4 becomes unreliable. We thus compare mode-based prediction intervals and mean-based prediction intervals under an assumed regression model in a different way as we describe next. Under each considered regression model, following maximum likelihood estimation based on the observed data $\mathcal{D} = \{(Y_i, \mathbf{X}_i), i = 1, \dots, n\}$, we compute an estimated mean residual standard deviation given by $\hat{\sigma} = [n^{-1} \sum_{i=1}^n \{Y_i - \hat{\mu}(\mathbf{X}_i)\}^2]^{1/2}$. Then a mode-based prediction interval is formulated as $\mathcal{PI}_\theta(\mathbf{X}_i, k) = [\hat{\theta}(\mathbf{X}_i) - k\hat{\sigma}, \hat{\theta}(\mathbf{X}_i) + k\hat{\sigma}]$, and a mean-based prediction interval is given by $\mathcal{PI}_\mu(\mathbf{X}_i, k) = [\hat{\mu}(\mathbf{X}_i) - k\hat{\sigma}, \hat{\mu}(\mathbf{X}_i) + k\hat{\sigma}]$, for some positive constant k . Unlike the prediction intervals constructed in Section 4.4, now with k and the MLE for $\boldsymbol{\Omega}$ given, these prediction intervals are of the same width and center at the corresponding central tendency measure. It is of interest to compare $\mathcal{PI}_\theta(\cdot, k)$ and $\mathcal{PI}_\mu(\cdot, k)$ in regard to their coverage probabilities, which we estimate using empirical coverage probabilities obtained from a leave-one-out cross validation procedure similar to that used in Section 4.4. That is, under each assumed regression model, the empirical coverage probability of, say, $\mathcal{PI}_\theta(\mathbf{X}_i, k)$, is defined as $n^{-1} \sum_{i=1}^n I\{Y_i \in \mathcal{PI}_\theta^{(-i)}(\mathbf{X}_i, k)\}$, where $\mathcal{PI}_\theta^{(-i)}(\mathbf{X}_i, k)$ is the mode-based prediction interval obtained using data \mathcal{D}_{-i} , for $i = 1, \dots, n$.

Under an assumed regression model, with k and $\hat{\sigma}$ given, a higher empirical coverage probability of a prediction interval indicates better predictive performance of the corresponding central tendency measure. Table 5 reports these coverage probabilities under the three considered regression models. It is worth pointing out that comparing these probabilities across

Table 5: Empirical coverage probabilities of mode-based prediction intervals, $\mathcal{PI}_\theta(\cdot, k)$, and mean-based prediction intervals, $\mathcal{PI}_\mu(\cdot, k)$, under each regression model for the compositional data

k	Beta mean model		Beta mode model		GBP mode model	
	\mathcal{PI}_θ	\mathcal{PI}_μ	\mathcal{PI}_θ	\mathcal{PI}_μ	\mathcal{PI}_θ	\mathcal{PI}_μ
0.1	0.083	0.042	0.069	0.056	0.111	0.083
0.2	0.167	0.181	0.194	0.167	0.194	0.139
0.5	0.403	0.389	0.417	0.389	0.417	0.486

different regression models is less meaningful because $\hat{\sigma}$ differs from one model to the other. Comparing the mode-based prediction interval and the mean-based prediction interval with a fixed width under each regression model in Table 5, one can see that the former usually yields a higher coverage probability than the latter when k is small.

6 Discussion

We propose two classes of regression models for studying the association between a bounded response and covariates via inferring the conditional mode of the response. Among all existing regression methodology, only a small subset of them are designed for mode regression, and an even smaller collection of them are in the parametric paradigm. The two mode regression models proposed in our study contribute new regression platforms for association studies when a bounded response is of interest. Under each proposed mode regression model, we have developed model diagnostic tools to detect various forms of inadequate parametric assumptions.

Besides allowing the mode to depend on covariates, one may consider covariate-dependent shape parameter $m(\mathbf{X})$ to expand the class of mode regression models. A more flexible family of mode regression models can be formulated as mixtures of beta or GBP distributions, which will allow inclusion of multimodal distributions. When an assumed mode regression model approximates the underlying truth reasonably well, we expect more effective variable selection procedures based on these mode regression models when comparing with exist-

ing non-/semi-parametric mean-/mode-based variable selection procedures. Hence, variable selection based on parametric mode regression models is an exciting direction of further exploration.

The family of GBP distributions is a rare distribution family that directly includes the mode in the parameterization, which makes it especially suitable for mode regression. If, unlike responses in our current study, the support of the response is unknown, then we have additional parameter(s) in the GBP density relating to the support, resulting in a non-regular model. In this case, maximum likelihood estimation can break down, or leads to estimators that do not possess properties one usually sees in an MLE under a regular model (Cheng and Amin, 1983). Parameter estimations and properties of MLEs for parameters in a non-regular GBP regression model demand systematic investigations.

Supplementary Materials

The online Supplementary Materials contains the following additional information: S1: algorithm for estimating p -value for the GBP score test; S2: additional results for simulation studies; S3: additional results for real data applications.

Acknowledgments

Data collection and sharing for this project was funded by the Alzheimer’s Disease Neuroimaging Initiative (ADNI) (National Institutes of Health Grant U01 AG024904) and DOD ADNI (Department of Defense award number W81XWH-12-2-0012). ADNI is funded by the National Institute on Aging, the National Institute of Biomedical Imaging and Bioengineering, and through generous contributions from the following: AbbVie, Alzheimers Association; Alzheimers Drug Discovery Foundation; Araclon Biotech; BioClinica, Inc.; Biogen; Bristol-Myers Squibb Company; CereSpir, Inc.; Cogstate; Eisai Inc.; Elan Pharmaceuticals, Inc.; Eli Lilly and Company; EuroImmun; F. Hoffmann-La Roche Ltd and its affiliated company

Genentech, Inc.; Fujirebio; GE Healthcare; IXICO Ltd.; Janssen Alzheimer Immunotherapy Research & Development, LLC.; Johnson & Johnson Pharmaceutical Research & Development LLC.; Lumosity; Lundbeck; Merck & Co., Inc.; Meso Scale Diagnostics, LLC.; NeuroRx Research; Neurotrack Technologies; Novartis Pharmaceuticals Corporation; Pfizer Inc.; Piramal Imaging; Servier; Takeda Pharmaceutical Company; and Transition Therapeutics. The Canadian Institutes of Health Research is providing funds to support ADNI clinical sites in Canada. Private sector contributions are facilitated by the Foundation for the National Institutes of Health (www.fnih.org). The grantee organization is the Northern California Institute for Research and Education, and the study is coordinated by the Alzheimers Therapeutic Research Institute at the University of Southern California. ADNI data are disseminated by the Laboratory for Neuro Imaging at the University of Southern California.

References

- Atkinson, A. C. (1987). *Plots, Transformations, and Regression: An Introduction to Graphical Methods of Diagnostic Regression Analysis*. Oxford University Press.
- Bamford, S. P., Rojas, A. L., Nichol, R. C., Miller, C. J., Wasserman, L., Genovese, C. R., and Freeman, P. E. (2008). Revealing components of the galaxy population through non-parametric techniques. *Monthly Notices of the Royal Astronomical Society*, 391(2):607–616.
- Boos, D. D. and Stefanski, L. A. (2013). *Essential statistical inference: theory and methods*, volume 120. Springer Science & Business Media.
- Chen, Y.-C., Genovese, C. R., Tibshirani, R. J., Wasserman, L., et al. (2016). Nonparametric modal regression. *The Annals of Statistics*, 44(2):489–514.
- Cheng, R. and Amin, N. (1983). Estimating parameters in continuous univariate distribu-

- tions with a shifted origin. *Journal of the Royal Statistical Society: Series B (Methodological)*, 45(3):394–403.
- Cox, D. R. and Hinkley, D. V. (1979). *Theoretical statistics*. Chapman and Hall/CRC.
- Damien, P., Walker, S., et al. (2017). Bayesian mode regression using mixtures of triangular densities. *Journal of Econometrics*, 197(2):273–283.
- deToledo Morrell, L., Stoub, T., Bulgakova, M., Wilson, R., Bennett, D., Leurgans, S., Wu, J., and Turner, D. (2004). Mri-derived entorhinal volume is a good predictor of conversion from mci to ad. *Neurobiology of aging*, 25(9):1197–1203.
- Devanand, D., Pradhaban, G., Liu, X., Khandji, A., De Santi, S., Segal, S., Rusinek, H., Pelton, G., Honig, L., Mayeux, R., et al. (2007). Hippocampal and entorhinal atrophy in mild cognitive impairment: prediction of alzheimer disease. *Neurology*, 68(11):828–836.
- Einbeck, J. and Tutz, G. (2006). Modelling beyond regression functions: an application of multimodal regression to speed–flow data. *Journal of the Royal Statistical Society: Series C (Applied Statistics)*, 55(4):461–475.
- Ferrari, S. and Cribari-Neto, F. (2004). Beta regression for modelling rates and proportions. *Journal of Applied Statistics*, 31(7):799–815.
- García, C. B. G., Pérez, J. G., and Rambaud, S. C. (2009). The generalized biparabolic distribution. *International Journal of Uncertainty, Fuzziness and Knowledge-Based Systems*, 17(03):377–396.
- Grantham, J. H. and Velbel, M. A. (1988). The influence of climate and topography on rock-fragment abundance in modern fluival sands of the southern blue ridge mountains, north carolina. *Journal of Sedimentary Research*, 58(2):219–227.
- Hall, P. (1992). On global properties of variable bandwidth density estimators. *The Annals of Statistics*, pages 762–778.

- Hämäläinen, A., Tervo, S., Grau-Olivares, M., Niskanen, E., Pennanen, C., Huuskonen, J., Kivipelto, M., Hänninen, T., Tapiola, M., Vanhanen, M., et al. (2007). Voxel-based morphometry to detect brain atrophy in progressive mild cognitive impairment. *Neuroimage*, 37(4):1122–1131.
- Hotelling, H. (1931). The generalization of student's ratio. *Ann. Math. Statist.*, 2(3):360–378.
- Jack, C. R., Petersen, R. C., Xu, Y. C., O'Brien, P. C., Smith, G. E., Ivnik, R. J., Boeve, B. F., Waring, S. C., Tangalos, E. G., and Kokmen, E. (1999). Prediction of ad with mri-based hippocampal volume in mild cognitive impairment. *Neurology*, 52(7):1397–1397.
- Jauhiainen, A. M., Pihlajamäki, M., Tervo, S., Niskanen, E., Tanila, H., Hänninen, T., Vanninen, R. L., and Soininen, H. (2009). Discriminating accuracy of medial temporal lobe volumetry and fmri in mild cognitive impairment. *Hippocampus*, 19(2):166–175.
- Kemp, G. C. and Silva, J. S. (2012). Regression towards the mode. *Journal of Econometrics*, 170(1):92–101.
- Killiany, R., Hyman, B., Gomez-Isla, T., Moss, M., Kikinis, R., Jolesz, F., Tanzi, R., Jones, K., and Albert, M. (2002). Mri measures of entorhinal cortex vs hippocampus in preclinical ad. *Neurology*, 58(8):1188–1196.
- Kueper, J. K., Speechley, M., and Montero-Odasso, M. (2018). The Alzheimers disease assessment scale–cognitive subscale (ADAS-Cog): modifications and responsiveness in pre-dementia populations. a narrative review. *Journal of Alzheimer's Disease*, (Preprint):1–22.
- Lee, M.-J. (1989). Mode regression. *Journal of Econometrics*, 542(3):337–349.
- Lee, M.-J. (1993). Quadratic mode regression. *Journal of Econometrics*, 57(1-3):1–19.
- Liu, J., Zhang, R., Zhao, W., and Lv, Y. (2013). A robust and efficient estimation method for single index models. *Journal of Multivariate Analysis*, 122:226–238.

- Rosen, W. G., Mohs, R. C., and Davis, K. L. (1984). A new rating scale for Alzheimer's disease. *The American journal of psychiatry*.
- Schmidt, M. (1996). *Key auditory verbal learning test: A handbook*. Western Psychological Services Los Angeles, CA.
- Tombaugh, T. N. and McIntyre, N. J. (1992). The mini-mental state examination: a comprehensive review. *Journal of the American Geriatrics Society*, 40(9):922–935.
- Van den Boogaart, K. G. and Tolosana-Delgado, R. (2013). *Analyzing compositional data with R*, volume 122. Springer.
- Wang, X., Chen, H., Cai, W., Shen, D., and Huang, H. (2017). Regularized modal regression with applications in cognitive impairment prediction. In Guyon, I., Luxburg, U. V., Bengio, S., Wallach, H., Fergus, R., Vishwanathan, S., and Garnett, R., editors, *Advances in Neural Information Processing Systems 30*, pages 1448–1458. Curran Associates, Inc.
- Whitwell, J. L., Shiung, M. M., Przybelski, S., Weigand, S. D., Knopman, D. S., Boeve, B. F., Petersen, R. C., and Jack, C. (2008). Mri patterns of atrophy associated with progression to ad in amnesic mild cognitive impairment. *Neurology*, 70(7):512–520.
- Yang, H. and Yang, J. (2014). A robust and efficient estimation and variable selection method for partially linear single-index models. *Journal of Multivariate Analysis*, 129:227–242.
- Yao, W. and Li, L. (2014). A new regression model: modal linear regression. *Scandinavian Journal of Statistics*, 41(3):656–671.
- Yu, K. and Aristodemou, K. (2012). Bayesian mode regression. *arXiv preprint arXiv:1208.0579*.
- Zhang, R., Zhao, W., and Liu, J. (2013). Robust estimation and variable selection for semi-parametric partially linear varying coefficient model based on modal regression. *Journal of Nonparametric Statistics*, 25(2):523–544.

Zhao, W., Zhang, R., Liu, J., and Lv, Y. (2014). Robust and efficient variable selection for semiparametric partially linear varying coefficient model based on modal regression. *Annals of the Institute of Statistical Mathematics*, 66(1):165–191.

Zhou, H. and Huang, X. (2019). Bandwidth selection for nonparametric modal regression. *Communications in Statistics-Simulation and Computation*, 48:968–984.

Parametric mode regression for bounded data

Haiming Zhou and Xianzheng Huang

Northern Illinois University and University of South Carolina

Supplementary Material

S1 Algorithm for estimating p -value for the GBP score test

This section provides additional information for Section 3.2 in the main paper.

- Step 1 Fit the assumed mode regression model to the observed data, $\mathcal{D} = \{(Y_i, \mathbf{X}_i), i = 1, \dots, n\}$. Denote by $\hat{\Omega}$ the resultant MLE for Ω .
- Step 2 Compute $Q(\hat{\Omega}; \mathcal{D})$ defined in Equation (3.3) in the main paper.
- Step 3 For $b = 1, \dots, B$, generate $Y_{i,b}$ from $\text{GBP}(\hat{\theta}(\mathbf{X}_i), \hat{m})$, where $\hat{\theta}(\mathbf{X}_i)$ and \hat{m} are MLEs for $\theta(\mathbf{X}_i)$ and m , respectively. This produces B sets of bootstrap data, $\mathcal{D}_b = \{(Y_{i,b}, \mathbf{X}_i), i = 1, \dots, n\}$, for $b = 1, \dots, B$.
- Step 4 Fit the assumed mode regression model to each bootstrap data set, \mathcal{D}_b , and obtain the MLE for Ω , denoted by $\hat{\Omega}_b$, for $b = 1, \dots, B$.
- Step 5 Compute the test statistic, $Q(\hat{\Omega}_b; \mathcal{D}_b)$, according to Equation (3.3) in the main paper, for $b = 1, \dots, B$.
- Step 6 Compute the estimated p -value defined by $B^{-1} \sum_{b=1}^B I\{Q(\hat{\Omega}_b; \mathcal{D}_b) > Q(\hat{\Omega}; \mathcal{D})\}$.

S2 Additional results for simulation studies

This section provides additional information for Section 4.4 in the main paper. Figure S1 provides prediction intervals when one assumes a beta mode model and data are generated from (B1) with $m = 10$.

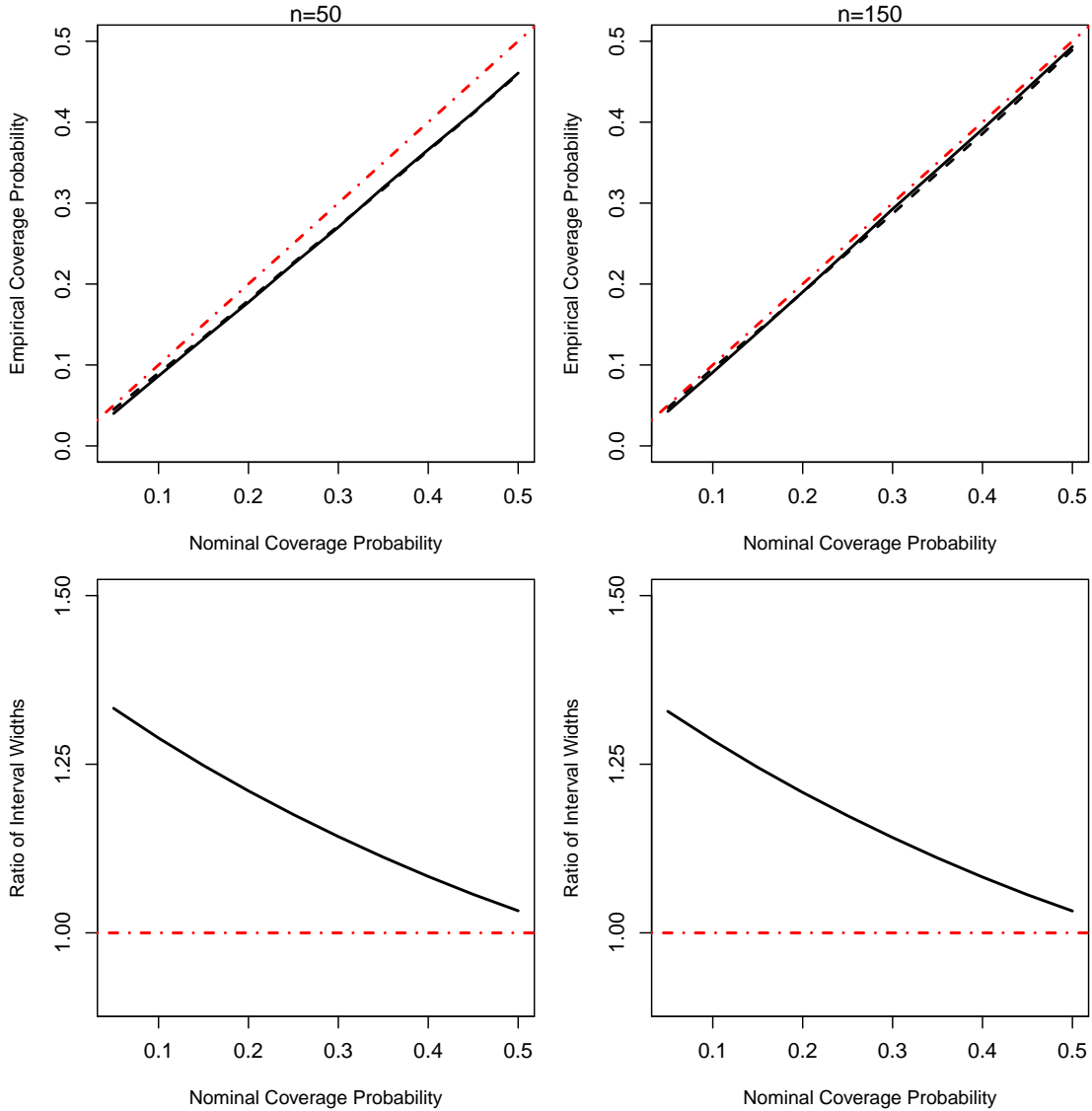


Figure S1: Prediction intervals based on data from the beta mode model in (B1) with $m = 10$. Top panels depict average empirical coverage probabilities (across 300 Monte Carlo replicates) of mode-based prediction intervals (solid lines), and those of mean-based prediction intervals (dashed lines) versus nominal coverage probabilities. Red dash-dotted lines are 45° reference lines. Lower panels depict ratios of the average width of mean-based prediction intervals over that of mode-based prediction intervals versus nominal coverage probabilities (solid lines). Red dash-dotted horizontal lines are reference lines at value one.

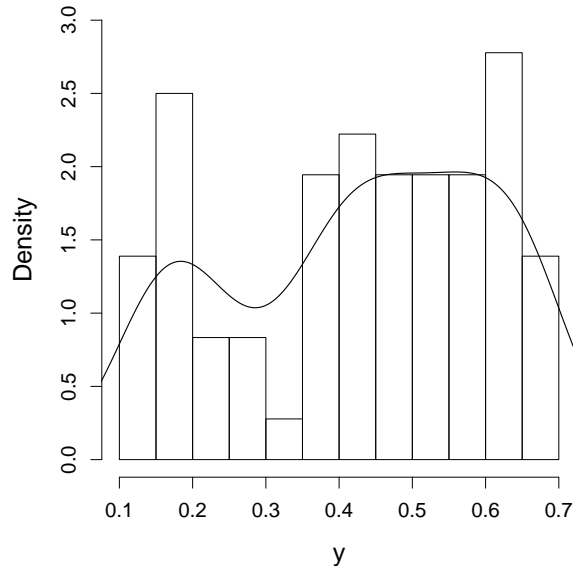


Figure S2: The histogram of the proportion response in the compositional data, overlaid with kernel density estimates for the marginal distribution of the response.

Table S1: Maximum likelihood estimates corresponding to each regression model for the compositional data. Numbers in parentheses are estimated standard errors associated with the MLEs.

Parameter	Beta mean model	Beta mode model	GBP mode model
β_0 (Intercept)	-0.1720 (0.0921)	-0.1838 (0.0946)	-0.1437 (0.1013)
β_1 (Position-s)	0.2071 (0.0448)	0.2135 (0.0462)	0.3074 (0.0544)
β_2 (Discharge)	0.0018 (0.0008)	0.0018 (0.0009)	0.0010 (0.0009)
β_3 (Relief)	-0.8111 (0.1096)	-0.8339 (0.1124)	-0.9883 (0.0916)
β_4 (Grain-f)	1.0952 (0.0421)	1.1217 (0.0434)	1.3059 (0.0331)
β_5 (Grain-m)	0.6932 (0.0390)	0.7105 (0.0401)	0.8260 (0.0377)
ϕ or $\log m$	95.9400 (15.92)	4.5426 (0.1692)	2.7370 (0.1144)

S3 Additional results for real data applications

This section provides additional information for Section 5 in the main paper. Figure S2 provides the histogram of the responses for the compositional data. Table S1 reports the maximum likelihood estimates corresponding to each regression model for the compositional data.